

Iterative Bleaching Extends Multiplexity (IBEX) imaging facilitates simultaneous identification of all cell types in the vertebrate retina

Aanandita Kothurkar^{1,§}, Gregory S. Patient^{1,§}, Nicole C. L. Noel¹, Colin J. Chu^{1,*}, Ryan B. MacDonald^{1,*}

§ These authors contributed equally to this work

*Co-corresponding senior authors: CJC (colin.chu@ucl.ac.uk) and RBM (ryan.macdonald@ucl.ac.uk)

¹Institute of Ophthalmology, University College London, London EC1V 9EL, UK

Keywords: Retina, immunohistochemistry, zebrafish, development, neurons, glia

ABSTRACT

The vertebrate retina is a complex multicellular tissue made up of distinct neuron types and glia, arranged in a stereotypic layered organisation to facilitate vision. Understanding how these cell types come together to form precise circuits during development requires the ability to simultaneously discriminate between multiple cell types and their spatial position in the same tissue. Currently, we have a limited capacity to resolve all constitutive cell types and their relationships to one another, due to our limited ability to combine multiple cellular markers or antibodies. To extend this capacity, we have adapted a highly multiplexed immunohistochemistry technique known as Iterative Bleaching Extends Multiplexity (IBEX) and applied it to the development of the zebrafish retina. IBEX allows for multiple rounds of cellular labelling to be performed before integration of the imaging data with open-source software, thereby facilitating visualisation of multiple markers on the same tissue section for analysis. We have optimised fluorescent micro-conjugation of known antibody markers with sequential imaging and bleaching to label the complete zebrafish retina with up to 11 cell-specific antibodies. We have further adapted the IBEX technique to be compatible with fluorescent transgenic reporter lines, *in situ* hybridisation chain reaction (HCR), and wholemount immunohistochemistry. Finally, we have applied IBEX at multiple stages of retinal development to study the spatial and temporal relationships between glia cells and neurons during development, demonstrating progressive specialisation of retinal cell types consistent with previously described histogenesis. Ultimately, these techniques can be applied to any tissue in zebrafish to rapidly explore multiple cell types and biological processes in single tissue samples.

INTRODUCTION

Tissues are made up of multiple cell types with regional and cell-specific molecular differences. To understand the multicellular composition, and how they are altered during development, ageing and/or disease, we must visualise the complete cellular landscape. This relies on the accessibility of techniques to assay or discriminate between multiple cell types across an entire tissue using their transcriptomes, epigenomes, and/or proteomes as features to define cell states or interactions in whole tissues (Choi *et al.*, 2023). However, these techniques remain in refinement and are costly to adapt for individual tissues of choice. As such, developing methods to multiplex existing, optimised and widely available techniques are critical to maximise cellular studies in any tissue from a wide variety of model organisms. Modern techniques, such as single-cell RNA-sequencing, can identify cell-specific molecular changes in individual cells on a large scale – however, the spatial organisation of these cells is lost in processing and must be mapped back onto the tissue to maximise their value. In contrast, immunohistochemistry (IHC) techniques allow visualisation of cellular proteins expressed in specific cell types in their undisturbed locations and thus provide spatial information. However, the number of antibody markers and, by consequence, the amount of information that can be obtained from a single tissue sample is limited by the number of fluorophores which can be imaged at one time. This is particularly relevant where few antibodies are validated and many are raised in the same host (e.g. rabbit), and so cannot be detected at the same time. Therefore, developing techniques to map the expression of multiple genes onto a tissue will enhance our ability to understand cellular state, behaviour, and function in any tissue.

The retina is the light-detecting tissue at the back of the eye, comprised of several different types of neurons and glia. Retinal structure has been well-characterised since its early description by anatomists such as Cajal, who used dye labels to identify individual cell types and their organisation based on their unique locations and morphologies (Cajal, 1893). The highly

organised retina is made up of five main neuronal cell types and a principal glia cell type called Müller glia (MG) (Fig. 1). Photoreceptors are the light-sensitive cells that synapse onto interneurons (horizontal cells, bipolar cells, and amacrine cells) which in turn, relay and modulate the signal and synapse with output neurons (retinal ganglion cells) that connect the retina to visual centres in the brain. These cells are organised into three discrete cell layers (outer nuclear layer, inner nuclear layer, and ganglion cell layer) separated by two synaptic neuropils (outer and inner plexiform layers) and form relatively simple circuits (Masland, 2012). The zebrafish retina has been a useful model to study of development and disease as it has a conserved organisation and cellular composition with other vertebrates (Avanesov and Malicki, 2010). Furthermore, it is an ideal CNS tissue to image *in vivo* as it is transparent during embryogenesis, develops rapidly (functional by 5 days post fertilisation (dpf) (Patterson *et al.*, 2013), and has a full complement of cell-specific fluorescent reporter lines to visualise every cell type in the tissue (reviewed in Malicki *et al.*, 2016). Further, there are a large number of antibodies with neuronal and glial specificity to discriminate different cell types and visualise morphology in the zebrafish retina (such as Yazulla and Studholme, 2001). However, studies of retinal development or disease remain constrained by our limited ability to combine these antibodies to visualise multiple cell types and directly assay cellular relationships or states in the same tissue.

Here, we overcome these challenges by adapting Iterative Bleaching Extends Multiplexity (IBEX) to zebrafish (Fig. 2). IBEX is a technique developed in mouse and human tissues that allows simultaneous visualisation of up to 60 markers on a single tissue sample (Radtke *et al.*, 2020), thereby providing large-scale, detailed multicellular spatial analysis of tissue. It relies on fluorescently conjugated primary antibodies to enable use of multiple antibodies raised in the same species while avoiding cross-reactivity and permits bleaching of signal to conduct sequential rounds of immunolabelling. First, we validated “micro-conjugations” whereby a small volume of antibody is directly linked to fluorescent dyes to overcome the critical issue of multiple

antibodies raised in the same species. Importantly, these fluorophores can be bleached and are compatible with multiple rounds of IHC required for the IBEX technique. Using IBEX, we then labelled every cell type in the retina with 11 specific antibody markers. We enhanced the capabilities of the IBEX technique by pairing with cell-specific transgenic reporter lines, wholemount IHC, and *in situ* hybridisation chain reaction (HCR) in zebrafish. Finally, we use IBEX to describe the development of two key cell types in the retina: photoreceptors and MG. The techniques described here will be valuable for any zebrafish tissue and are applicable to any other study where multiplexed IHC is required.

MATERIALS AND METHODS

Table 1. Antibodies used for immunohistochemistry and IBEX.

REAGENT OR RESOURCE	HOST	SOURCE	IDENTIFIER	DILUTION
Primary antibodies				
α -GS	Mouse	Proteintech	Cat. No. CL488-66323	1:50
α -PKC- β	Rabbit Polyclonal	Proteintech	Cat. No. 12919-1-AP	1:50
α -PCNA	Rabbit polyclonal	Proteintech	Cat. No. 24036-1-AP	1:50
α -M/L opsin	Rabbit	Millipore Merck	Cat. No. AB5405	1:50
α -HuC/D	Mouse	Invitrogen	Cat. No. A21271	1:100
α -GNAT2	Rabbit polyclonal	MBL	Cat. No. PM075	1:75

α -LCP1	Rabbit polyclonal	Proteintech	Cat. No. 13025-1-AP	1:50
α -RLBP1	Rabbit polyclonal	Proteintech	Cat. No. 15356-1-AP	1:50
α -RPE65	Rabbit polyclonal	Proteintech	Cat. No. 17939-1-AP	1:25
α -Ribeye-A	Rabbit polyclonal	Gift from Teresa Nicholson	NA	1:500
α -GFAP	Mouse	Biolegend	Cat. No. 837508	1:50
α -Zo1	Mouse Monoclonal	Life technologies	Cat. No. 339100	1:150
α - Zrf-1	Mouse Monoclonal	ZIRC	Cat. No. ZDB-ATB- 081002-46	1:25
α -Calretinin	Rabbit polyclonal	Swant	Cat. No. 7697	1:150
α -ARR3	Rabbit	Merck	Cat. No. AB15282	1:50
α -Carbonic anhydrase	Rabbit polyclonal	ABCAM	Cat. No. ab196835	1:50
α -Calbindin	Rabbit	Swant	Cat. No. CB38a	1:50
α -UV opsin	Rabbit polyclonal	Kerafast	Cat. No. EJH013	1:50
α -Blue opsin	Rabbit polyclonal	Kerafast	Cat. No. EJH012	1:50
α -GFP	Rabbit polyclonal	Invitrogen	Cat: A11122	1:500

α-Zpr1	Mouse	ZIRC	ZDB-ATB-081002-43	1:200
α-PRPH2	Rabbit polyclonal	Proteintech	Cat. No. 18109-1-AP	1:200
α-1D4	Mouse monoclonal	Santa Cruz Biotechnology	Cat. No. sc-57432	1:50
Secondary antibodies				
α-Rabbit Alexa Fluor™ 647	Goat	Invitrogen	Cat. No. A-21244	1:1000
α-Rabbit Alexa Fluor™ 546	Goat	Invitrogen	Cat. No. A-11035	1:1000
α-Mouse Alexa Fluor™ 546	Goat	Invitrogen	Cat. No. A-11030	1:1000
α-Mouse Alexa Fluor™ 647	Goat	Invitrogen	Cat. No. A-21235	1:1000
α-Chicken Alexa Fluor™ 488	Goat	Invitrogen	Cat. No. A-11039	1:1000
Other markers				
Lectin PNA		Invitrogen	Cat. No. L21409	
DAPI		Invitrogen	Cat. No. D1306	1:1000
Conjugation kits				
FlexAble CoraLite® 488 Antibody Labeling Kit for Rabbit IgG		Proteintech	Cat. No. KFA001	
FlexAble CoraLite® Plus 550 Antibody Labeling Kit for Rabbit IgG		Proteintech	Cat. No. KFA002	
FlexAble CoraLite® Plus 647 Antibody Labeling Kit for Rabbit IgG		Proteintech	Cat. No. KFA003	

FlexAble CoraLite® Plus 750 Antibody Labeling Kit for Rabbit IgG		Proteintech	Cat. No. KFA004	
FlexAble CoraLite® Plus 550 Antibody Labeling Kit for Mouse IgG1		Proteintech	Cat. No. KFA022	
FlexAble CoraLite® Plus 647 Antibody Labeling Kit for Mouse IgG1		Proteintech	Cat. No. KFA023	
ReadiLink™ Rapid iFluor® 594 Antibody Labeling Kit		AAT	Cat. No. 1230-AAT	

Animals

Adult zebrafish were housed in the animal facility at the University College London Institute of Ophthalmology on a 14:10 hour light/dark cycle at 28°C, following previously established husbandry protocols (Westerfield, 1993). Experimental procedures were conducted in accordance with the UK Home Office Animals (Scientific Procedures) Act 1986 (zebrafish project license PPL: PP2133797, held by R.B.M). Embryos were obtained by light-induced spawning, collected in E3 buffer (5 mM NaCl, 0.17 mM KCl, 0.33 mM CaCl₂, 0.33 mM MgSO₄) with/without methylene blue, and maintained in an incubator at 28.5°C till use.

Zebrafish strains

Wildtype zebrafish embryos (ABTL/Tübingen) were used for the adaptation of the IBEX technique on section IHC, wholemount IHC and combined HCR/IHC. Tg(*GFAP:GFP*) (Bernardos and Raymond, 2006), Tg(*vsx1:GFP*)^{nns5} (Kimura, Satou and Higashijima, 2008), Tg(*TP1:Venus-Pest*)

(Ninov, Borius and Stainier, 2012), *Tg(tp1bglob:eGFP-CAAX)* (Kugler *et al.*, 2023) and *Tg(ptf1a:dsRed)^{ia6}* (Jusuf *et al.*, 2012) were used to optimise the protocol for IBEX using transgenics. *Tg(rho:YFP)^{gm500}* (White *et al.*, 2017), *Tg(tp1bglob:eGFP-CAAX)* embryos were used at different timepoints to study development of neurons and glia.

Preparation of retinal sections

Zebrafish embryos at the desired stages were overdosed with 0.4% Tricaine and fixed in 4% paraformaldehyde overnight at 4°C. They were washed 3 times for 5 min in PBS and then immersed in 30% sucrose in PBS and allowed to sink overnight. Samples were embedded in OCT (Sigma Aldrich, Cat. No. SHH0024) and frozen at -80°C. SuperFrost™ Plus Adhesion Microscope Slides (Epredia, Cat. No. J1800AMNZ) were coated evenly with 5 µL chrome alum gelatin (Newcomer Supply, Part# 1033C) and dried in an incubator at 60°C for one hour, to minimise loss of tissue over multiple rounds of immunolabelling. Retinal sections of the embedded embryos were sectioned onto these slides at a thickness of 12-14 µm using a cryostat (Leica CM1950) and left at room temperature (RT) to dry overnight. Slides were then stored at -80°C.

Antibody micro-conjugation

Each antibody (Table 1) was tested with the FlexAble micro-conjugation kits at the recommended concentration (0.5 µg) per slide. However, this did not label cells efficiently in retinal sections. Doubling the concentration of primary antibody was found to stain tissue more effectively. 1 µg of each primary antibody was combined with 2 µL of linker protein for the desired fluorophore, and the volume was made up to 16 µL with the provided buffer. This solution was incubated for 5 minutes in the dark at RT, and then 4 µL of quencher was added and left to incubate in the dark at RT for a further five minutes, according to the manufacturer's protocol. The entire reaction volume for each antibody was used for subsequent steps.

IBEX technique

This method is an adapted version of the original IBEX protocol (Radtke *et al.*, 2020) and an overview is given in Fig. 2. The sections were rehydrated in PBS for 5 minutes at RT. Antigen retrieval was then performed by heating the slides for 20 minutes in 10 mM sodium citrate (pH 6). This step quenched the signal in most of the GFP transgenic lines tested. The transgene can be boosted in later rounds of immunolabelling using a primary antibody against GFP. The sections were blocked for 1 hour in block solution (10% goat serum, 1% BSA, 0.8% Triton X, 0.1% Tween, made up with PBS) at RT. Primary antibodies were conjugated to fluorophores as described above. The slides were incubated with of the first round of antibodies, diluted appropriately in block solution, at 4°C overnight. Following three 20-minute washes with PBS, secondary antibodies were added, if needed. Slides were then incubated at RT for two hours or overnight in 4°C and washed after with PBS three times for 10 minutes. Slides were mounted in Fluoromount G mounting media (Cat. No. 00-4958-02, Invitrogen) and imaged on a Leica THUNDER imager, Leica SP8 confocal microscope, or Zeiss LSM 900 inverted confocal using 4-5 channels: 405, 488, 550, 647 and 750 nm.

After image acquisition, slides were placed in a 50 mL falcon tube filled with PBS and left until the coverslip fell off, and then washed three times to remove the mounting media. Fluorophores were quenched by incubating slides in 150 µL of lithium borohydride (LiBH₄, 16949-15-8, STREM) solution (1-2 mg/mL) under direct light (234632226972, Savage Universal PGLSA-KIT SM light) for 30 minutes. The slide was then washed three times for 10 minutes before the next round of antibodies was added and steps were repeated as above.

IBEX for combined *in situ* HCR/IHC on sections

HCR probes for *cyp26a1* and *vsx1* were kindly gifted by Takeshi Yoshimatsu, while the probe set for *glula* was designed using a custom script (Trivedi and Powell, unpublished) and ordered from Life Technologies, ThermoFisher. HCR amplifiers (Alexa Fluor 488, Alexa Fluor 546, and Alexa Fluor 647), and buffers (hybridisation, wash, and amplification) were purchased from Molecular

Instruments (<https://www.molecularinstruments.com/>). A published *in situ* HCR protocol (Choi *et al.*, 2018) was adapted for retinal zebrafish sections. Slides were rehydrated in PBS for 5 minutes and then treated with 250 μ L proteinase K (20 μ g/mL) for 10 minutes at RT. They were washed twice with PBS + 0.1% Tween (PBST) and post-fixed with 250 μ L of 4% paraformaldehyde for 20 minutes at RT. Slides were washed 3 times for 5 minutes with PBST and incubated in 150 μ L of probe hybridisation buffer at 37°C for 30 minutes. Sections were then incubated overnight at 37°C in probe solution (4 μ L of each probe set, made up to 150 μ L in probe hybridisation buffer). Excess probes were removed by washing slides 4 times for 15 minutes in probe wash buffer at 37°C, and then 2 times for 5 minutes with 5X SSCT buffer at RT. Slides were pre-amplified in 150 μ L of amplification buffer for 30 minutes at RT. 4 μ L each of hairpin 1 and hairpin 2 amplifier were snap cooled by heating to 95°C for 90 seconds and cooling to RT. These were then added to the slides in 150 μ L of amplification buffer and incubated overnight at RT in the dark. Slides were washed 4 times for 5 minutes in 5X SSCT buffer and mounted in Fluoromount G media. Sections were imaged on the Zeiss LSM 900 with a 40x immersion oil objective (Na 1.1) using 4 channels: 405, 488, 546, and 647 nm. After image acquisition, slides were heated to 60°C in sodium citrate (pH 6) for 20 minutes to quench fluorophores. IHC was carried out on sections as described above.

IBEX for wholemount IHC

Wildtype embryos were treated with 0.0045% phenylthiourea from 6 hpf to prevent pigment formation and at 5 dpf, were overdosed with 0.4% Tricaine and fixed in 4% paraformaldehyde overnight at 4°C. They were washed in PBST and heated in 10mM sodium citrate (pH 6) at 70°C for 15 minutes. Samples were washed twice for 10 minutes in PBST, twice for 5 minutes in distilled water and incubated with ice cold acetone for 20 minutes at -20°C. This was followed by three 5 min washes in PBS and incubation in blocking solution (10% goat serum, 0.8% Triton X-100, 1% BSA in PBST) for 2 hrs at RT. Micro-conjugation of the antibodies was carried out as described above, doubling the volume of antibody used for sections. Embryos were incubated in antibody

solution with DAPI, diluted with blocking solution, at RT overnight with gentle agitation at room temperature. After three 1-hour washes in PBS + 1% Tween, embryos were mounted in molten 1% low melting point agarose in PBS, in a glass bottomed dish. Once hardened, they were covered with 1X PBS and imaged on the Zeiss LSM 900 with a 40x immersion oil objective (Na 1.1) using 4 channels: 405, 488, 546, and 647 nm.

Quenching of fluorophores

Fluorophores react differently to bleaching with LiBH₄, and therefore, we used several different methods to bleach signal between rounds of labelling. CoraLite micro-conjugated antibodies bleached after 30 minutes of LiBH₄ treatment under bright light. The same antibodies required 2 hours of incubation in LiBH₄ solution to observe reduction in signal in WM IHC. In cases where Alexa Fluor 555 secondary antibody was used, 30 minutes of heating at 60°C in sodium citrate solution (pH 6) was needed to quench the fluorescence. For transgenic lines, antigen retrieval by boiling slides in sodium citrate solution (pH 6) for 20 minutes quenched the fluorescent protein, but when boosted with the anti-GFP primary and Alexa Fluor secondary antibodies, the signal was not reduced even after antigen retrieval. Hence, fluorophores must be individually tested to assess suitability for use with IBEX, and ones that do not show reduction in signal used in the last round of immunolabelling.

Image processing and alignment

Imaging parameters such as stack size, number of steps, step size, scan speed, and resolution were kept consistent across all rounds of imaging. Once all rounds were completed, Imaris (Oxford Instruments) was used to process the images. Brightness, contrast, and colours were adjusted and filters, such as Gaussian, were applied where appropriate. Once all images were processed, the SITK-IBEX registration code (Radtke *et al.*, 2020) was used to register them, using

DAPI as the alignment channel. Maximum projection images were obtained using the snapshot feature while in 3D viewer or by using the orthogonal slicer tool.

RESULTS

Direct conjugation to fluorophores facilitates labelling with multiple antibodies raised in the same host on the same tissue

A major hurdle in IHC is labelling with multiple antibodies raised in the same animal (e.g. rabbit) as it would not be possible to distinguish between the antibodies using traditional secondary antibodies. To overcome this limitation, we used “micro-conjugation” reactions (see Methods) to directly link primary antibodies with distinct fluorophores, avoiding use of secondary antibodies and gaining the flexibility to label each antibody with a fluorophore of choice (Fig. S1). To ensure there was no cross-reactivity or quenching of signal due to competitive antibody binding, we conjugated the rabbit GNAT2 antibody, which labels cone photoreceptors in the zebrafish retina, with four different fluorophores. Using confocal microscopy, we observed robust signal for each of the fluorophores in the photoreceptor layer with no noticeable loss of signal due to multiple conjugated antibodies against the same protein (Fig. S1).

It is critical for the multiplexity of the IBEX technique to be able to bleach the fluorescent signals between rounds of IHC. We demonstrate that CoraLite fluorophores can be successfully bleached using lithium borohydride (LiBH_4) and show a near complete loss of signal and no autofluorescence in any channel post bleaching (Fig. S1). Next, to determine if we could concurrently label cells with four distinct rabbit polyclonal antibodies, we micro-conjugated each with different fluorophores and conducted a single round of IHC and imaging. We labelled photoreceptors with GNAT2, bipolar cell synapses with Ribeye-A, bipolar cell terminals with PKC- β , and MG with RLBP1 (Fig. 3); we were able to visualise these concurrently without any cross

reactivity. Therefore, using micro-conjugations we can reliably visualise and quench the fluorophores of antibodies raised in the same species on the same tissue section.

Adapting IBEX to label all cell types in the zebrafish retina

To label every major cell type in the retina with IHC, we designed a panel of markers against proteins expressed in each cell type of the zebrafish retina composed of micro-conjugated antibodies and directly conjugated antibodies. First, we optimised each antibody for use with micro-conjugation by testing for bright, specific labelling in single IHC tissue staining and bleaching (see Materials and Methods). In some cases, directly conjugated antibodies did not show sufficient staining to be easily visualised by standard IHC or they were not successfully bleached by LiBH₄. Fortunately, a standard antigen retrieval step was sufficient to bleach and enhance the staining for these antibodies. Using three rounds of iterative bleaching followed by standard confocal imaging, we labelled each cell type in the retina using 11 markers and DAPI in the same tissue section (Fig. 4). In each IHC round, we used DAPI to label nuclei, which is used for alignment and the ultimate integration of multiple markers on the same tissue as it does not bleach. This provides a consistent fiducial landmark for image registration. The open source SimpleITK registration software (Radtke *et al.*, 2020) for registration of confocal Z-stacks is effective at increasing the alignment of DAPI signal between the three rounds (Fig. S2) and allows channels from the different rounds to be merged. As such, we developed panels of combinatorial fluorescent antibody labels against each cell type in the retina, imaged each panel in successive imaging rounds after quenching of fluorophores, and integrated the data onto a single image file (Fig. 4A). To increase the rate at which we can acquire data from multiple samples, we also optimised IBEX and the panel of markers for an epifluorescence imaging system with onboard deconvolution (Leica THUNDER). This allows for a large area of tissue to be imaged quickly and

effectively over multiple rounds to visualise 9 antibodies and a lectin stain on the same tissue (Fig. S3).

IBEX is compatible with cell-specific transgenic reporter lines

Identifying reliable antibodies for specific cell types or cellular processes of interest in zebrafish can be challenging. The zebrafish has a wealth of cell-specific transgenic reporter lines that drive transgene expression in each population of retinal cell. These have been valuable tools to characterise the development and degeneration of retinal cell types in many studies (Fadool, 2003; Bernardos and Raymond, 2006; Zolessi *et al.*, 2006; Kimura, Satou and Higashijima, 2008; Vitorino *et al.*, 2009; Almeida *et al.*, 2014). Therefore, we aimed to assess whether we could combine IBEX with existing transgenic lines to enhance our multiplex toolbox. To incorporate transgenic reporter lines into the IBEX technique, it is ideal for the fluorescent protein to bleach and make the channel available for future imaging rounds. We tested whether endogenous fluorescent protein signals could be quenched and then re-labelled with fluorescent protein-specific antibodies by IHC. We tested several transgenic lines containing cytosolic or membrane-targeted GFP, YFP, or RFP. We found that both cytosolic and membrane-tagged GFP bleached after antigen retrieval methods (Fig. S4). However, we could not bleach the RFP or YFP transgenic lines with LiBH₄ in combination with intense light nor sodium citrate antigen retrieval (Fig. S4C, D). Thus, it is possible to pair IBEX with transgenic lines, although this should be tested on a case-by-case basis to determine whether endogenous fluorescent proteins can be bleached, and subsequent labelling rounds adjusted accordingly.

IBEX can be combined with fluorescent *in situ* hybridisation

Antibodies specific for a cell type or protein of interest can be limited in zebrafish. As an alternative, *in situ* hybridisation chain reaction (HCR) is a robust method to label mRNA of interest in zebrafish (Choi *et al.*, 2010, 2016, 2018). HCR has been previously combined with IHC in the zebrafish (Howard *et al.*, 2021; Ibarra-García-Padilla *et al.*, 2021; Ćorić *et al.*, 2023), however, these are limited by the number of channels available in a single labelling round on standard microscopes. We next tested whether HCR methods to label mRNA would be compatible with IBEX, such that we could conduct a multiplex HCR followed by bleaching, IHC and integration of labelling techniques on the same retina. For this, we performed HCR for three genes of interest: *cyp26a1*, *glula*, and *vsx1*. The expression of these genes is known to be specific to different retinal cell populations: MG (*cyp26a1* and *glula*) and bipolar cells (*vsx1*) (Fig. 5A-A'''). We then attempted to quench the signal of these fluorophores using LiBH₄ treatment. However, we did not observe a significant reduction in signal for Alexa Fluor 555 (Fig. 5B-B''') We were able to bleach this signal using the antigen retrieval technique (Fig. 5B''') before conducting a subsequent round of IHC with MG and bipolar cell antibody markers (Fig C-C'''). We overlaid these two rounds of imaging, one HCR and one IHC, which allowed us to visualise expression of the three transcripts of interest and confirm co-localisation with different retinal cell populations (Fig. 5D-D'''). Hence, combining *in situ* HCR with IHC using IBEX is a powerful technique to identify expression patterns of genes of interest by localizing gene expression to different immunolabelled cell types.

Wholemout IBEX facilitates whole tissue labelling in zebrafish

The relatively small size of the zebrafish retina and the ability to treat the fish to make the eyes optically transparent lends itself to wholemount IHC (Inoue and Wittbrodt, 2011; Santos, Monteiro and Luzio, 2018). This technique facilitates the study of cell structure and shape in its native conformation and overcomes the potential disruption of cell morphology and tissue damage introduced by cryosectioning. However, the hurdle of visualizing multiple cell types in the same

sample remains. Therefore, we tested whether the micro-conjugated antibody staining and bleaching is compatible with thicker tissues in wholemount IHC before carrying out the IBEX protocol. We tested the protocol by immunolabelling MG and photoreceptors with two different antibodies each, over two successive rounds of imaging (Fig. 6A,A',C,C'). Micro-conjugated antibodies penetrated the tissue and specifically labelled photoreceptors and MG. Treatment with LiBH_4 successfully bleached the signal of each of the fluorophores between rounds (Fig. 6B). The SimpleTK registration software allowed us to combine the images and observe the co-localisation of antibodies labelling Müller glia and photoreceptors, respectively, across different rounds of immunofluorescence (Fig. 6E,E',F). Therefore, wholemount IHC when combined with IBEX allows 3D labelling of multiple cell types and alignment of their spatial relationships to one another between rounds.

IBEX facilitates the characterisation of retinal histogenesis and patterning

The retina has a stereotyped histogenesis whereby retinal neurons and glia are born and specified in distinct temporal sequence during retinogenesis (Agathocleous and Harris, 2009). Specification of the zebrafish retina begins at 24 hours post fertilisation (hpf) as a retinal primordium, completing histogenesis by 73 hpf (Easter and Nicola, 1996) with robust vision beginning at 5 dpf. We used this well-characterised developmental pattern to determine the utility of IBEX to describe cellular morphologies in the highly dynamic developing retina. We focussed on two main cell types: photoreceptors, which have five distinct subtypes that are challenging to visualise simultaneously by traditional methods, and MG, due to their highly dynamic morphological changes across retinal development. We used cryosections at different key timepoints of retinal development to accomplish this.

Zebrafish photoreceptors undergo rapid development, with light-sensitive opsin mRNA expression detectable by 60 hpf (Robinson, Schmitt and Dowling, 1995). Zebrafish are tetrachromats: they have rods and four cone photoreceptor subtypes, maximally sensitive to ultraviolet (UV), blue, green, and red light. Different photoreceptor types are identifiable by specific markers; however, traditional methods make it challenging to label all photoreceptor subtypes such that they are distinguishable from one another. We combined antibody labelling with a transgenic line with fluorescently labelled rods (Tg(*rho*:YFP) line) to label all photoreceptors with subtype resolution in the developing zebrafish retina at three stages (3, 4, and 5 dpf) (Fig. 7). We distinguished between the cone subtypes by utilising antibodies against UV, blue, and red opsin (via 1D4), as well as arrestin 3a (with *zpr-1*). *Zpr-1* labels both red and green cones; green cones can therefore be identified as cells that are arrestin 3a-positive but do not stain for red opsin (Fig. S5). At 3 dpf, developing cone photoreceptors stain with GNAT2 and *zpr-1* (Fig. 7A''), and have small outer segments labelled with antibodies for PRPH2, UV opsin, blue opsin, and red opsin (Fig 7A''', A'''). Most of the cones with discernible outer segments were observed in the central retina. Few newly developed YFP-positive rods can also be observed in the retinal periphery. By 4 dpf, cones appear more morphologically mature with lengthened outer segments (Fig. 7B-B'''). As mentioned, zebrafish cones are functional by 5 dpf and the animals begin to perform complex visually mediated behaviours, such as prey capture (Patterson *et al.*, 2013). Corresponding with this, 5 dpf zebrafish cones have visually longer outer segments compared to 4 dpf with a tapered morphology (Fig. 7C-C'''). Furthermore, there appear to be phagosomes in the RPE staining for *zpr-1*, GNAT2, UV opsin, and PRPH2, suggesting that there is outer segment disc shedding at this stage.

During development, nascent MG cells begin as simple unbranched radial cells at 2.5 dpf, before morphologically elaborating to a mature, highly branched structure by 5 dpf (Williams *et al.*, 2010; MacDonald *et al.*, 2015; Wang *et al.*, 2017). MG are among the last retinal cell types to mature,

integrating into neuronal circuits when neurons are undergoing robust synaptogenesis (Cepko *et al.*, 1996). To determine MG specification relative to development of other retinal neurons and inner plexiform layer (IPL) formation, we used markers for MG: Zrf-1 (recognising Gfap), glutamine synthetase (GS), and the Tg(*Tp1:EGFP-CAAX*) transgenic reporter line, which labels retinal progenitors and MG (MacDonald *et al.*, 2015; Kugler *et al.*, 2023). We labelled amacrine cells and retinal ganglion cells with HuC/D, horizontal cells with CA-1, bipolar cells with PKC- β , and synapse formation with Ribeye-A. We observed retinal progenitors at 2 dpf (Fig. 8A-A'') labelled by the GFP transgene, corresponding to retinal ganglion cell (RGC) specification below the IPL, before MG genesis and onset of MG cell body basal migration at 2.5 dpf. MG are labelled by the transgene and *zrf1* at 2.5 dpf, but GS labelling is not yet apparent (Fig. 8B-B''). At this point, the nascent IPL is present, as evidenced by the separation of the HuC/D signal and presence of ribbon synapses (Ribeye-A) (Fig. 8B',B'''). From this timepoint, horizontal cells are visible, marked by carbonic anhydrase (CA) below the outer plexiform layer (Fig. 8B',C',D'). At 3 dpf, IPL expansion and bipolar cell terminal stratification is seen (Ribeye-A and PKC- β), along with the beginning of organisation of the IPL into clear sub-laminae (Fig 8C'-C'''). Additionally, MG cell bodies have migrated to their final positions (Fig. 8C'') and are marked by GS labelling. By 5 dpf, the ribbons are organised into discrete layers in the IPL, with a visible separation between the ON and OFF layers and MG have elaborated processes into this layer to provide homeostatic support functions (Fig 8D-D'''). As such, we used IBEX to describe retinal histogenesis, neuron migration and patterning relative to glial specification and morphogenesis across retinal development in the zebrafish. In conclusion, we were able to employ the IBEX technique and specifically designed antibody panels to describe multiple cell types at key stages of retinal development and explore their cellular relationships not possible with traditional methods.

DISCUSSION

There is a lack of tools in zebrafish to discriminate between more than three or four cell types in a tissue simultaneously. Here, we have adapted the IBEX technique to work in zebrafish tissues and optimised the methodology to be compatible with cell specific fluorescent reporter lines, wholemount IHC and *in situ* HCR. Further, we employed IBEX to describe the relationships between glial cells and neurons and explore the complete complement of photoreceptor subtypes in the developing retina. Therefore, IBEX is a robust method to multiplex markers and characterise cellular and molecular processes in the zebrafish.

Antibody panel design and considerations

To maximise the potential of IBEX, we developed panels to label as many cell types as possible in each round of IBEX. Careful planning is required to design panels of markers (antibodies/lectins) to be used based on previous individual reactions and bleaching tests. The brightest and least efficiently bleached markers, for instance lectins or transgenes, were used in later or, ideally, last round to minimise the potential for significant leftover signal. Similarly, the weakest markers were used in early panels to increase the likelihood of strong signal detection. It is important to note that certain fluorophores are more amenable to bleaching than others. We ensured that the fluorophores which have been validated to bleach in the original protocol (Radtko et al., 2020) were used and any new fluorophores, such as the CoraLite[®] Plus, were tested for bleaching prior to use in IBEX (Fig 3F). It is possible to use secondary antibodies in IBEX. This may be required for antibodies that fail to efficiently label via micro-conjugation. However, these secondaries must be incorporated into the first round of the IBEX if recognising a species from which multiple antibodies within the designed panel are raised, as subsequent rounds using antibodies raised in that same species will lead to cross-reactivity; in the case that there is a single antibody from a specific species within the panel, the antibody can be incorporated into any round using secondary antibodies. For most fluorophores, incubation with LiBH₄ before washing was

sufficient for bleaching the fluorophore. However, in some cases it required an antigen retrieval step (i.e. heating in sodium citrate) which efficiently quenches fluorophores. Importantly, after the antigen retrieval and IBEX procedure on zebrafish retinal tissue, the nuclei appeared qualitatively similar across three rounds of IHC and imaging (Fig S2) and were easily aligned using the SimpleITK registration software.

Potential of IBEX and multiplexing in other tissues and species

IBEX is a powerful addition to the zebrafish toolkit and can be applied to study development and degeneration in various organs. It could be used in conjunction with cell death markers like Caspase-3 or TUNEL dyes to localise cell death/degeneration to specific cell types. Zebrafish are also a powerful model for regeneration research (Gemberling *et al.*, 2013), and the ability to visualise multiple markers simultaneously can be applied to identify cells involved in regeneration/wound healing. Finally, methods for rapid genetic screening have recently been developed in zebrafish using multiple guide RNAs to induce high rates of biallelic knockout of the gene of interest in injected embryos (crispants) (Kroll *et al.*, 2020). IBEX can be utilised to efficiently characterise phenotypes in these crispants, which are often limited in number by injection capacity and efficiency.

IBEX can also be applied to other species of animals where multiple cell-specific antibodies, fluorescent reporter transgenes and *in situ* hybridisation techniques are available. However, these techniques and antibody panels will need to be validated on a case-by-case basis. These methodologies, some developed here, will be especially valuable where multiple different markers are required to confirm the identity of a cell, such as immunological studies. This means that large amounts of information can be gleaned from small quantities of precious tissue, a huge benefit for study of rare species or tissue that is difficult to access. It is also beneficial in newly established model organisms, in which fluorescent transgenesis is not routinely possible. Labelling multiple markers on the same tissue will also have important implications for animal ethics and 3Rs

(Replacement, Reduction and Refinement) initiatives as the number of animals required for statistically significant phenotypic data is greatly reduced. Performing multiple rounds of IHC on the same tissue produces rich datasets where the interactions between multiple cell types can be explored. As such, multiplexing techniques are not only powerful for data collection and exploring cellular relationships in whole tissues but also critical for efforts to reduce animal numbers in experiments.

Limitations & future work

There were some limitations to the IBEX approach. Micro-conjugations can be unreliable on occasion (i.e. not all antibodies successfully conjugate), there is a need for a relatively large volume of validated primary antibody (although much less than when performing a primary conjugation), and the technique works most effectively when the protein in question is highly abundant. Hence, when used for proteins that have low expression or low affinity for antibodies, the concentrations may have to be increased over traditional methods. Many antibodies do not have their exact antigen identified or validated in non-mammalian systems, such as zebrafish. However, as we were only looking at broad cell type distributions, rather than targeted molecular events, validation of each antigen was not necessary for this study. When possible, we did utilise antibodies with known/validated antigens. When using unvalidated antibodies, we selected those that had conserved labelling patterns and included other methods – such as transgenic lines and *in situ* hybridisation – to complement the labelling and provide information about specificity. Transgenic lines with RFP/YFP that do not bleach (such as the Tg(*rho:YFP*) line used for the developmental series in Fig. 7) can still be used if required but would reduce the number of channels available for successive imaging rounds. Finally, there are likely limitations on the number of immunolabelling rounds that can be performed without tissue damage or visible residual signal from previous rounds. However, we have conducted four rounds of IBEX on retinal

cryosections and there has been no noticeable degradation of tissue integrity or signal loss. As such, it may be possible to >20 markers on a single zebrafish cryosectioned tissue, as there have been 20 rounds and 66 antibodies reported in human lymph nodes (Radtke *et al.*, 2020).

The IBEX technique is compatible with standard confocal as well as epifluorescence microscopy. Here, we principally used a standard confocal microscope with four excitation laser wavelengths (405, 488, 555, and 647) that allowed a maximum of three antibodies plus DAPI in each panel. However, this can be expanded upon if your microscope has additional spectral capabilities (e.g. tuneable or white light laser) and antibodies are visualised with additional fluorophores via conjugation or secondary antibodies. To this end, we also conducted IBEX using an epifluorescence microscope with Z-stack capabilities and expanded spectral excitation properties to visualise 10 markers on the same tissue (Fig. S3). As such, this technique will be applicable to any fluorescence microscopes available where multiple channels can be acquired on the same tissue.

Conclusions

In conclusion, we have adapted a highly multiplexed immunohistochemistry technique (IBEX) to visualise many targets in a single zebrafish retina sample. We have established a pipeline which can be used to carry out multiplexed imaging on multiple zebrafish tissue samples at different timepoints at once. We successfully modified the IBEX protocol to be compatible with *in situ* hybridisation chain reaction (HCR) as well as wholemount tissue and characterised cellular relationships in the developing retina across every cell type in the tissue. Therefore, this technique can be a powerful method to explore multicellular tissues in zebrafish, and potentially other model organisms.

ACKNOWLEDGEMENTS

We would like to thank Dr. Mariya Moosajee for the kind gift of *Tg(rho:YFP)^{gm500}* embryos, and Dr. Chintan Trivedi for allowing use of his custom HCR probe design script. This study was supported by BrightFocus Macular Degeneration Postdoctoral Fellowship to N.C.L.N., a Wellcome Trust Clinical Research Career Development Fellowship (224586/Z/21/Z) and Moorfields Eye Charity equipment grant to C.J.C and a BBSRC David Phillips Fellowship (BB/S010386/1) to R.B.M.

REFERENCES

- Agathocleous, M. and Harris, W.A. (2009) 'From Progenitors to Differentiated Cells in the Vertebrate Retina', *Annual Review of Cell and Developmental Biology*, 25(1), pp. 45–69. Available at: <https://doi.org/10.1146/annurev.cellbio.042308.113259>.
- Almeida, A.D. *et al.* (2014) 'Spectrum of Fates: a new approach to the study of the developing zebrafish retina', *Development*, 141(14), pp. 2912–2912. Available at: <https://doi.org/10.1242/dev.114108>.
- Avanesov, A. and Malicki, J. (2010) 'Analysis of the Retina in the Zebrafish Model', *Methods in cell biology*, 100, pp. 153–204. Available at: <https://doi.org/10.1016/B978-0-12-384892-5.00006-2>.
- Bernardos, R.L. and Raymond, P.A. (2006) 'GFAP transgenic zebrafish', *Gene Expression Patterns*, 6(8), pp. 1007–1013. Available at: <https://doi.org/10.1016/j.modgep.2006.04.006>.
- Cajal, S.R.Y. (1893) 'La retine des vertebres.', *Cellule*, 9, pp. 119–255.
- Cepko, C.L. *et al.* (1996) 'Cell Fate Determination in the Vertebrate Retina', *Proceedings of the National Academy of Sciences of the United States of America*, 93(2), pp. 589–595.
- Choi, H.M.T. *et al.* (2010) 'Programmable in situ amplification for multiplexed imaging of mRNA expression', *Nature Biotechnology*, 28(11), pp. 1208–1212. Available at: <https://doi.org/10.1038/nbt.1692>.
- Choi, H.M.T. *et al.* (2016) 'Mapping a multiplexed zoo of mRNA expression', *Development*, 143(19), pp. 3632–3637. Available at: <https://doi.org/10.1242/dev.140137>.
- Choi, H.M.T. *et al.* (2018) 'Third-generation in situ hybridization chain reaction: multiplexed, quantitative, sensitive, versatile, robust', *Development*, 145(12), p. dev165753. Available at: <https://doi.org/10.1242/dev.165753>.

Choi, J. *et al.* (2023) 'Spatial organization of the mouse retina at single cell resolution by MERFISH', *Nature Communications*, 14(1), p. 4929. Available at: <https://doi.org/10.1038/s41467-023-40674-3>.

Ćorić, A. *et al.* (no date) 'A fast and versatile method for simultaneous HCR, immunohistochemistry and EdU labeling (SHInE)'.

Easter, Jr., Stephen S. and Nicola, G.N. (1996) 'The Development of Vision in the Zebrafish (*Danio rerio*)', *Developmental Biology*, 180(2), pp. 646–663. Available at: <https://doi.org/10.1006/dbio.1996.0335>.

Fadool, J.M. (2003) 'Development of a rod photoreceptor mosaic revealed in transgenic zebrafish', *Developmental Biology*, 258(2), pp. 277–290. Available at: [https://doi.org/10.1016/S0012-1606\(03\)00125-8](https://doi.org/10.1016/S0012-1606(03)00125-8).

Gemberling, M. *et al.* (2013) 'The zebrafish as a model for complex tissue regeneration', *Trends in Genetics*, 29(11), pp. 611–620. Available at: <https://doi.org/10.1016/j.tig.2013.07.003>.

Howard, A.G. *et al.* (2021) 'An atlas of neural crest lineages along the posterior developing zebrafish at single-cell resolution', *eLife*, 10, p. e60005. Available at: <https://doi.org/10.7554/eLife.60005>.

Ibarra-García-Padilla, R. *et al.* (2021) 'A protocol for whole-mount immuno-coupled hybridization chain reaction (WICHCR) in zebrafish embryos and larvae', *STAR Protocols*, 2(3), p. 100709. Available at: <https://doi.org/10.1016/j.xpro.2021.100709>.

Inoue, D. and Wittbrodt, J. (2011) 'One for All—A Highly Efficient and Versatile Method for Fluorescent Immunostaining in Fish Embryos', *PLOS ONE*, 6(5), p. e19713. Available at: <https://doi.org/10.1371/journal.pone.0019713>.

Jusuf, P.R. *et al.* (2012) 'Biasing Amacrine Subtypes in the Atoh7 Lineage through Expression of Barhl2', *Journal of Neuroscience*, 32(40), pp. 13929–13944. Available at: <https://doi.org/10.1523/JNEUROSCI.2073-12.2012>.

Kimura, Y., Satou, C. and Higashijima, S. (2008) 'V2a and V2b neurons are generated by the final divisions of pair-producing progenitors in the zebrafish spinal cord', *Development*, 135(18), pp. 3001–3005. Available at: <https://doi.org/10.1242/dev.024802>.

Kroll, F. *et al.* (no date) 'A simple and effective F0 knockout method for rapid screening of behaviour and other complex phenotypes', *eLife*, 10, p. e59683. Available at: <https://doi.org/10.7554/eLife.59683>.

Kugler, E. *et al.* (2023) 'GliaMorph: a modular image analysis toolkit to quantify Müller glial cell morphology', *Development (Cambridge, England)*, 150(3), p. dev201008. Available at: <https://doi.org/10.1242/dev.201008>.

MacDonald, R.B. *et al.* (2015) 'Müller glia provide essential tensile strength to the developing retina', *The Journal of Cell Biology*, 210(7), pp. 1075–1083. Available at: <https://doi.org/10.1083/jcb.201503115>.

- Malicki, J. *et al.* (2016) 'Chapter 8 - Analysis of the retina in the zebrafish model', in H.W. Detrich, M. Westerfield, and L.I. Zon (eds) *Methods in Cell Biology*. Academic Press (The Zebrafish), pp. 257–334. Available at: <https://doi.org/10.1016/bs.mcb.2016.04.017>.
- Masland, R.H. (2012) 'The Neuronal Organization of the Retina', *Neuron*, 76(2), pp. 266–280. Available at: <https://doi.org/10.1016/j.neuron.2012.10.002>.
- Ninov, N., Borius, M. and Stainier, D.Y.R. (2012) 'Different levels of Notch signaling regulate quiescence, renewal and differentiation in pancreatic endocrine progenitors', *Development*, 139(9), pp. 1557–1567. Available at: <https://doi.org/10.1242/dev.076000>.
- Patterson, B.W. *et al.* (2013) 'Visually guided gradation of prey capture movements in larval zebrafish', *Journal of Experimental Biology*, 216(16), pp. 3071–3083. Available at: <https://doi.org/10.1242/jeb.087742>.
- Radtke, A.J. *et al.* (2020) 'IBEX: A versatile multiplex optical imaging approach for deep phenotyping and spatial analysis of cells in complex tissues', *Proceedings of the National Academy of Sciences of the United States of America*, 117(52), pp. 33455–33465. Available at: <https://doi.org/10.1073/pnas.2018488117>.
- Robinson, J., Schmitt, E.A. and Dowling, J.E. (1995) 'Temporal and spatial patterns of opsin gene expression in zebrafish (*Danio rerio*)', *Visual Neuroscience*, 12(5), pp. 895–906. Available at: <https://doi.org/10.1017/S0952523800009457>.
- Santos, D., Monteiro, S.M. and Luzio, A. (2018) 'General Whole-Mount Immunohistochemistry of Zebrafish (*Danio rerio*) Embryos and Larvae Protocol', *Methods in Molecular Biology (Clifton, N.J.)*, 1797, pp. 365–371. Available at: https://doi.org/10.1007/978-1-4939-7883-0_19.
- Vitorino, M. *et al.* (2009) 'Vsx2 in the zebrafish retina: restricted lineages through derepression', *Neural Development*, 4(1), p. 14. Available at: <https://doi.org/10.1186/1749-8104-4-14>.
- Wang, J. *et al.* (2017) 'Anatomy and spatial organization of Müller glia in mouse retina', *The Journal of Comparative Neurology*, 525(8), pp. 1759–1777. Available at: <https://doi.org/10.1002/cne.24153>.
- Westerfield, M. (1993) *The Zebrafish Book: A Guide for the Laboratory Use of Zebrafish (Brachydanio Rerio)*. M. Westerfield.
- White, D.T. *et al.* (2017) 'Immunomodulation-accelerated neuronal regeneration following selective rod photoreceptor cell ablation in the zebrafish retina', *Proceedings of the National Academy of Sciences*, 114(18), pp. E3719–E3728. Available at: <https://doi.org/10.1073/pnas.1617721114>.
- Williams, P.R. *et al.* (2010) 'In vivo development of outer retinal synapses in the absence of glial contact', *The Journal of Neuroscience: The Official Journal of the Society for Neuroscience*, 30(36), pp. 11951–11961. Available at: <https://doi.org/10.1523/JNEUROSCI.3391-10.2010>.
- Yazulla, S. and Studholme, K.M. (2001) 'Neurochemical anatomy of the zebrafish retina as determined by immunocytochemistry', *Journal of Neurocytology*, 30(7), pp. 551–592. Available at: <https://doi.org/10.1023/a:1016512617484>.

Zolessi, F.R. *et al.* (2006) 'Polarization and orientation of retinal ganglion cells in vivo', *Neural Development*, 1(1), p. 2. Available at: <https://doi.org/10.1186/1749-8104-1-2>.

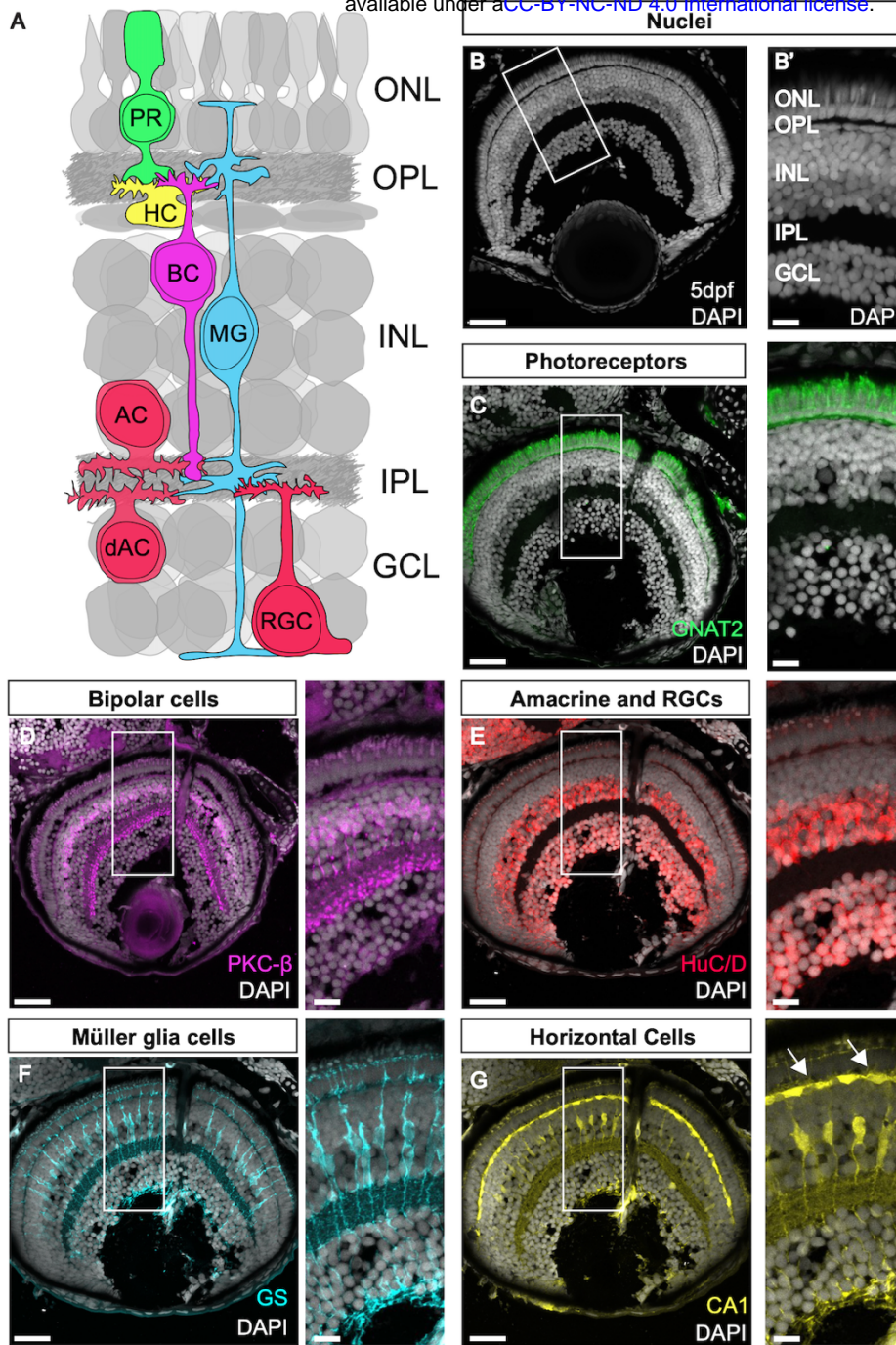


Figure 1. The retina is made up of highly organised layers composed of neurons and glia. (A) Schematic of the retina showing the layers and major cell populations with each cell type colour coded. (B) DAPI staining showing the nuclear layers of the retina. (B') Zoom of B. (C-G) Antibody staining for the main cell types in the zebrafish retina. Arrows in G show horizontal cells. OLM: outer limiting membrane, ONL: outer nuclear layer, OPL: outer plexiform layer, INL: inner nuclear layer, IPL: inner plexiform layer, GCL: ganglion cell layer. Scale bars - 25µm for whole retina, 10µm for zoom images.

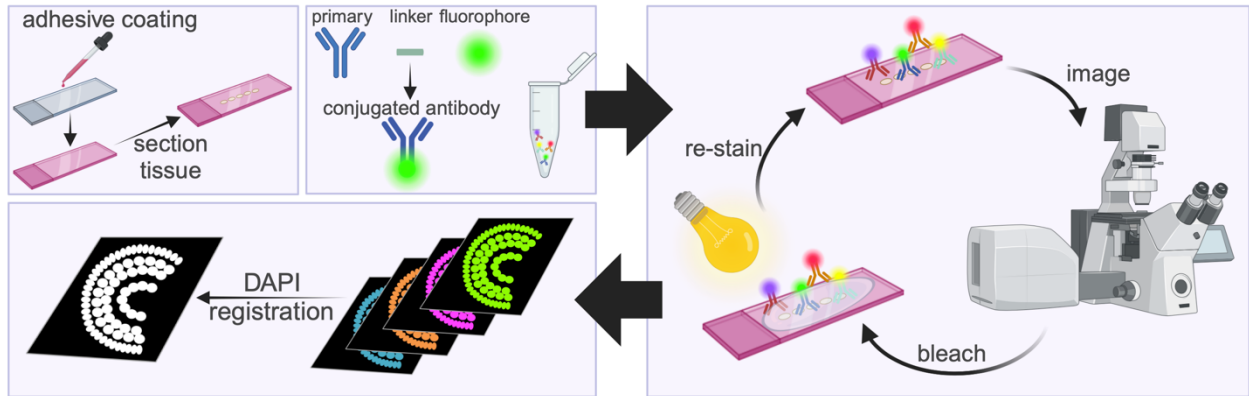


Figure 2. Schematic of the IBEX method. Slides are coated with chrome alum gelatin to prevent tissue lost, then tissue sectioned onto slides. Antibodies are micro-conjugated by mixing the primary antibody with a linker and fluorophore. The antibodies are applied to the slide, incubated, imaged, then bleached using bright light and lithium borohydride before being re-stained. After the imaging rounds are completed, nuclear stains (DAPI) are used to register the image, allowing for all stains to be visualised together.

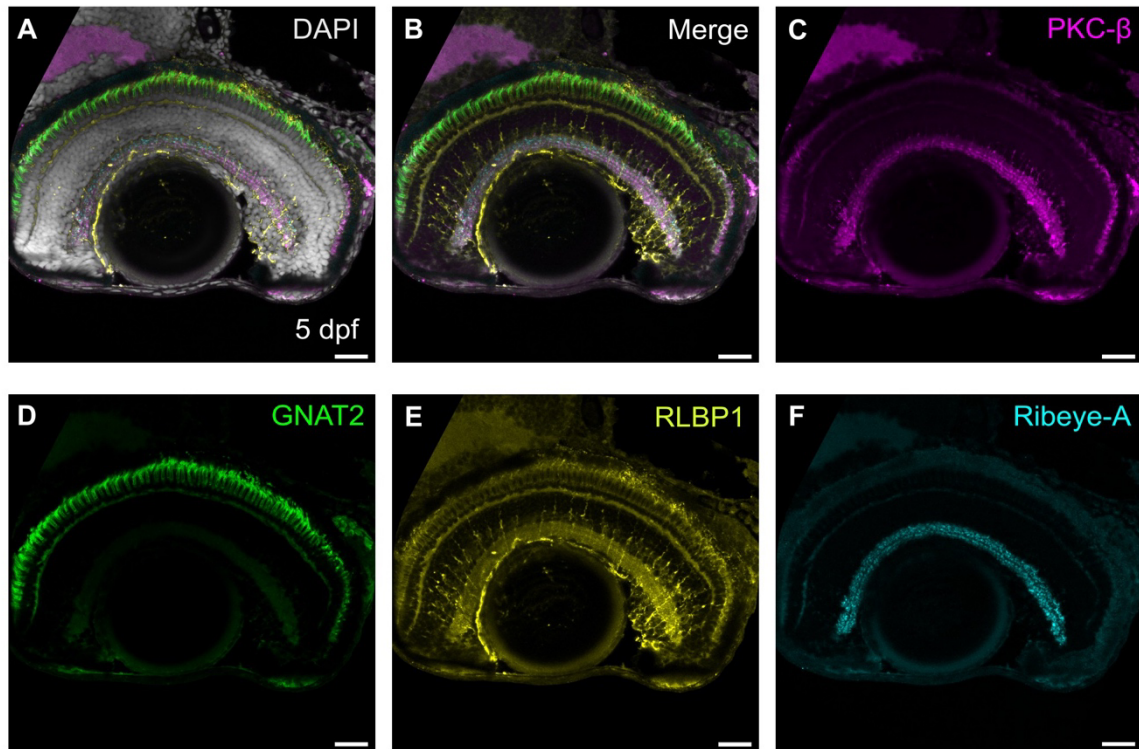


Figure 3. Direct conjugation to fluorophores facilitates multiple single species antibody labels on the same tissue. (A) Merged image of a single retinal section immunolabelled with four antibodies raised in rabbit: PKC- β (magenta), GNAT2 (green), RLBP1 (yellow), Ribeye-A (cyan), and nuclear stain DAPI (grey). (B) Merged image without DAPI. (C) Retinal section immunolabelled with PKC- β , marking bipolar cells. (D) Retinal section immunolabelled with GNAT2 marking cones. (E) Retinal section immunolabelled with RLBP1, marking Müller glia cells. (F) Retinal section immunolabelled with Ribeye-A marking ribbon synapses. Scale bars - 25 μ m.

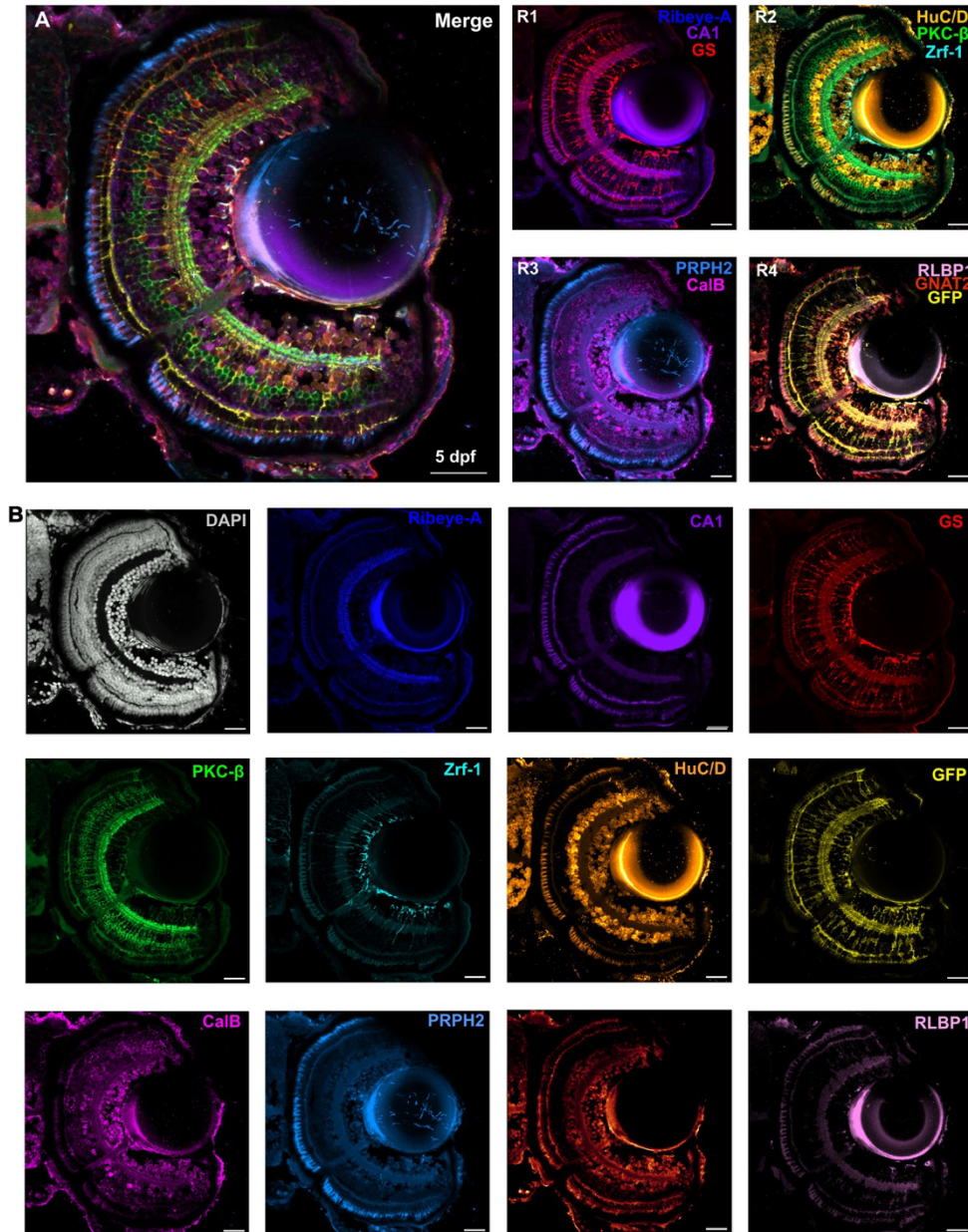


Figure 4. IBEX enables simultaneous labelling of all retinal cell types. (A) Confocal images of 5 dpf *Tg(tp1:eGFP:CAAX)* zebrafish retina showing different rounds of immunolabelling (R1-4) using IBEX and the merge composite image of each of these rounds. R1 was carried out using Alexa Fluor secondary antibodies, while other rounds used directly conjugated antibodies. (B) Confocal images showing each antibody used in (A) to immunolabel a single retinal section with DAPI and 11 different markers: Ribeye-A (dark blue), carbonic anhydrase (CA1, purple), glutamine synthetase (GS, red), PKC-β (green), Zrf-1 (cyan), HuC/D (orange), GFP transgene (yellow), calbindin (CalB, magenta), peripherin-2 (PRPH2, light blue), GNAT2 (orange), and RLBP1 (pink). Scale bars - 25μm.

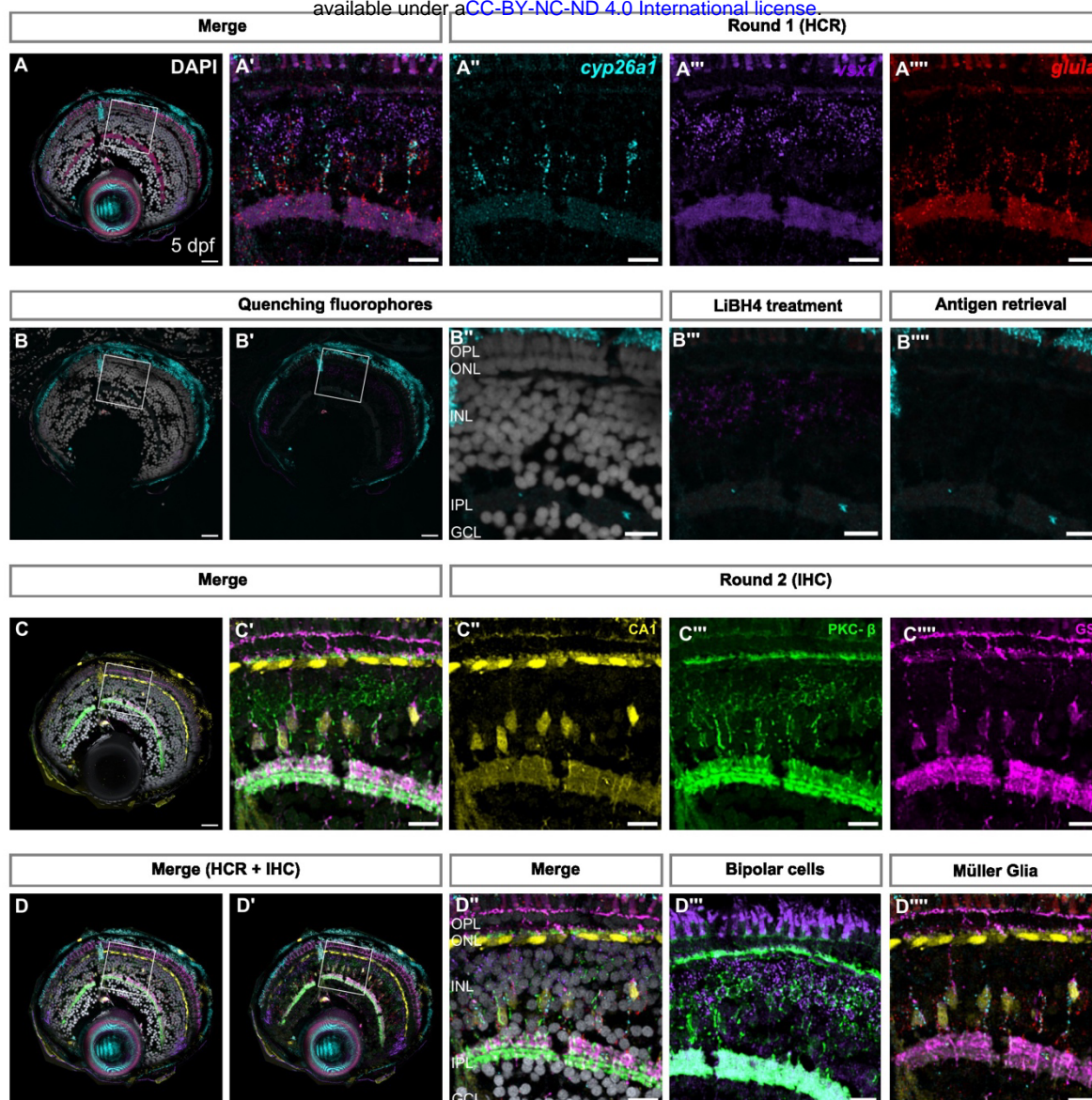


Figure 5. IBEX is compatible with fluorescent *in situ* hybridisation chain reaction. (A) Confocal images of retinal sections showing mRNA expression of *cyp26a1*, *glula*, and *vsx1*, using *in situ* hybridisation chain reaction (HCR). (A'-A''') Zoom on the region of interest indicated in (A). (B-B''') Confocal images showing reduced signal of Alexa Fluor-488 and Alexa Fluor-647, but not Alexa Fluor-555 after LiBH4 treatment. (B''') Heating in sodium citrate at 60°C causes inactivation of Alexa Fluor 555 as well as Alexa Fluor 488 and Alexa Fluor 647. (C) Confocal images of retinal sections immunolabelled with CA1 (yellow), PKC-β (green), and GS (magenta). (C'-C''') Zoom on region of interest indicated in (C). (D) SimpleITK registered image, showing overlay of both rounds of imaging, and overlay of *in situ* probes and antibodies detecting Müller glia and bipolar cells, respectively. (D''-D''') Zoom of region of interest shown in (D,D'). GCL: ganglion cell layer, IPL: inner nuclear layer, ONL: outer nuclear layer, OPL: outer plexiform layer. Scale bars - 25μm for whole retina, 10μm for zoom images.

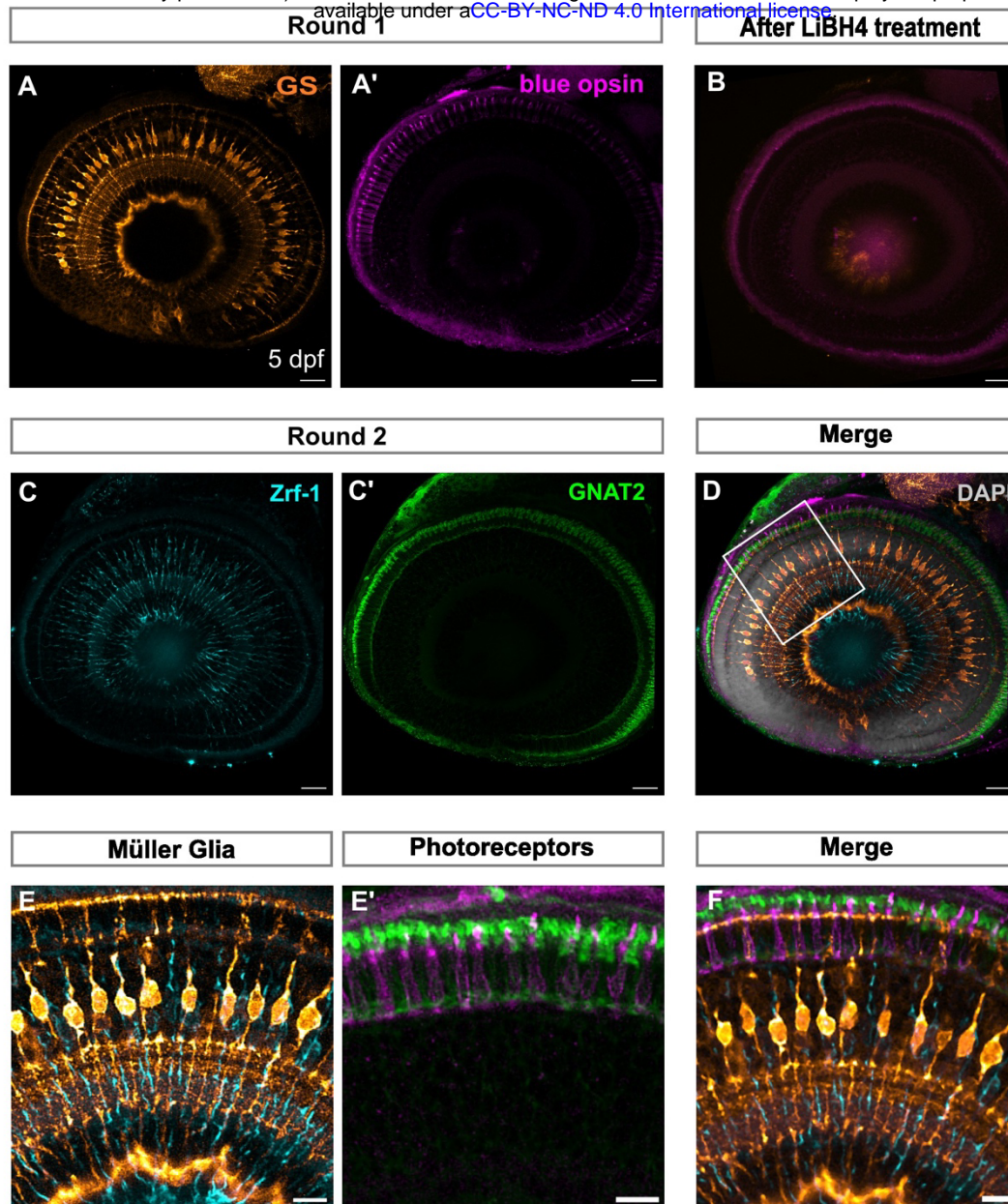


Figure 6. Wholemount IBEX facilitates whole tissue labelling in zebrafish (A,A') Confocal images of wholemount zebrafish larvae at 5 dpf immunolabelled with GS (orange) and blue opsin (magenta). (B) Tissue after bleaching with LiBH4 showing reduced signal of fluorophores CoraLite 488 and CoraLite 647. (C,C') Confocal images of the second round of immunolabelling to detect Zrf1 (cyan) and GNAT2 (green). (D) Merge of both rounds of immunolabelling using SimpleTK registration pipeline counterstained with DAPI (grey). (E) Overlap of MG markers GS and Zrf1 across round 1 and 2. (E') Overlap of photoreceptor markers blue opsin and GNAT2 across round 1 and 2. (F) Zoom in of (D), showing overlay of MG and photoreceptor labelling. dpf: days post fertilisation, MG: Müller glia. Scale bars - 25µm for whole retina, 10µm for zoom images.

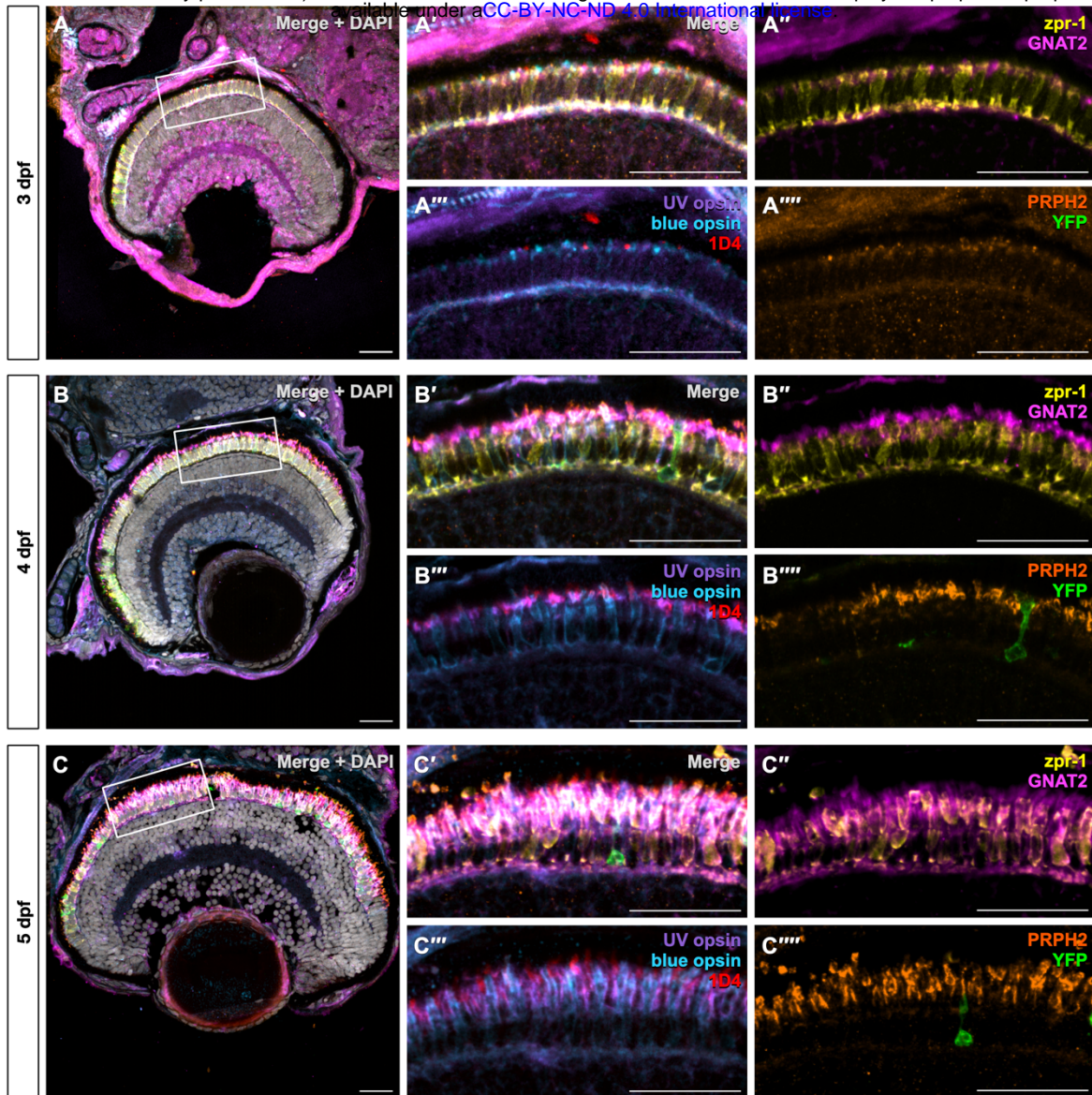


Figure 7. Visualisation of all photoreceptor subtypes during zebrafish development using IBEX. *Tg(rho:YFP)* embryos labelled with *zpr-1* (yellow), GNAT2 (pink), UV opsin (purple), blue opsin (blue), 1D4 (red), and PRPH2 (orange) at 3 (A), 4 (B), and 5 (C) dpf. YFP is shown in green. (A', B', C') Show zooms of photoreceptors with all labels merged, without DAPI; (A'', B'', C'') shows *zpr-1* and GNAT2 labelling; (A''', B''', C''') shows UV, blue, and red opsin (1D4) labelling; and (A''', B''', C''') shows PRPH2 labelling and YFP. (A) 3 dpf retinas have small, newly developing outer segments visible by UV opsin, blue opsin, red opsin (1D4), and PRPH2 labelling. Entire cone cell bodies are visible by GNAT2 labelling, while red and green cone cell bodies are visible by arrestin 3a (*zpr-1*) labelling. Newly formed rods are visible at the periphery of the retina by YFP labelling. (B) 4 dpf embryos have longer outer segments with increased PRPH2 staining, indicative of disc structure. (C) 5 dpf embryos have long outer segments that are visibly starting to taper into more of a “cone-like” morphology. dpf: days post fertilisation. Scale bars - 25µm.

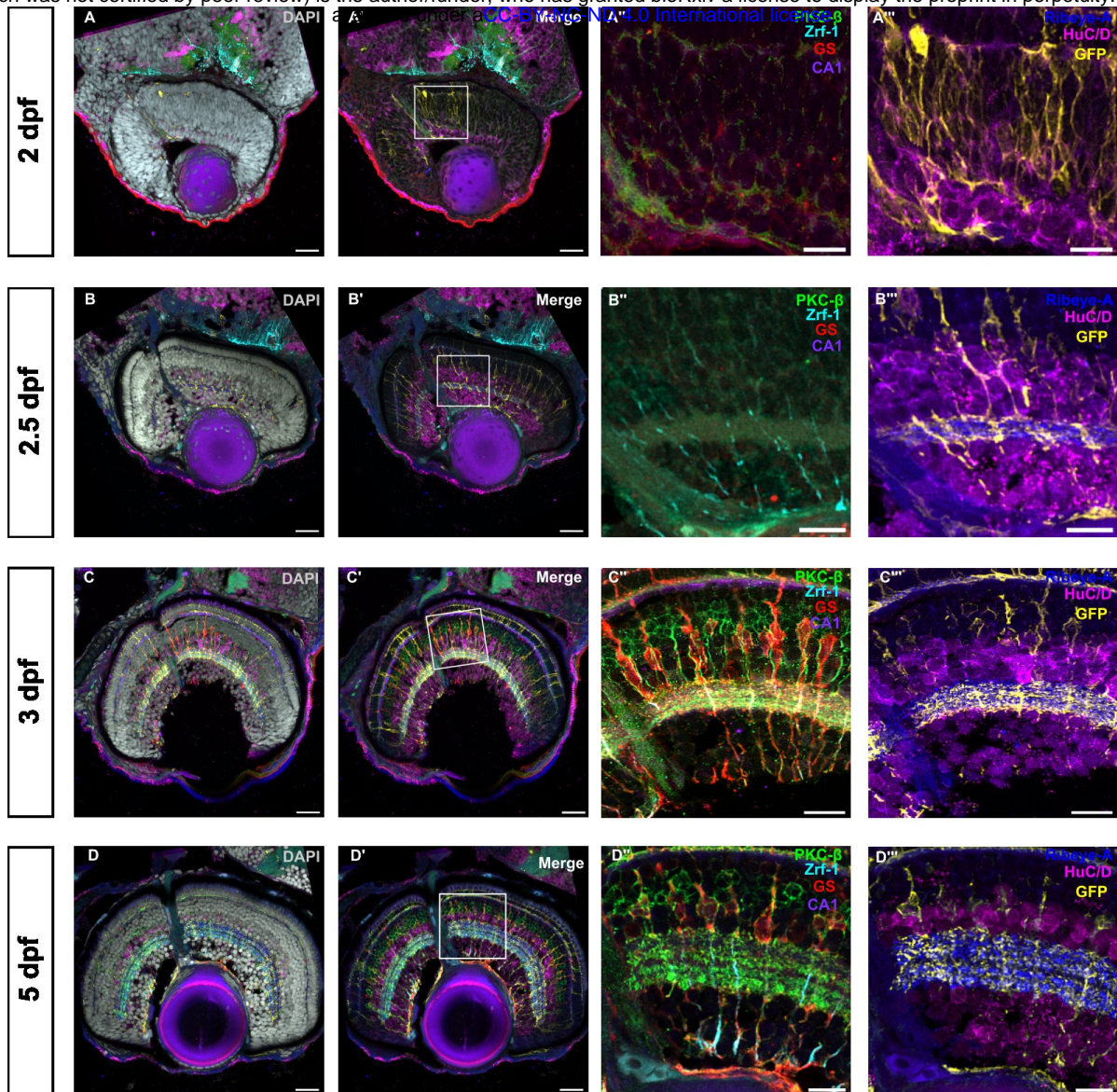


Figure 8. Visualisation of glial and neuronal development in the zebrafish retina. Confocal images of the developing zebrafish retina from 2 dpf to 5 dpf immunolabelled with DAPI and 7 different markers using IBEX over 3 rounds of immunolabelling with IBEX. A, B, C, D show merge of all 7 markers with nuclear stain DAPI, while A', B', C', D' show the same overlay of markers without DAPI. A'', B'', C'', D'' show the first 2 rounds of immunolabelling of bipolar cells (PKC- β , green), glial intermediate filaments (Zrf-1, cyan), horizontal cells (CA1, purple) and Müller glia (GS, red) at different timepoints. A''', B''', C''', D''' show the last round of immunolabelling of ribbon synapses (Ribeye-A, blue), amacrine & ganglion cells (HuC/D, magenta) and Müller glia (eGFP transgene, yellow) at different, crucial timepoints of retinal development (2, 2.5, 3, and 5 dpf) showing retinal progenitors in (A-A'''). (B-B''') shows nascent IPL and Müller glia formation. In (C-C''' and D-D'''), IPL sublamination and Müller glia elaboration is evident. dpf: days post fertilisation, IPL: inner plexiform layer. Scale bars - 25 μ m for whole retina, 10 μ m for zoom images.